

## Research Article

# Investigation of the Catalytic Performance of a Novel Nickel/Kit-6 Nanocatalyst for the Hydrogenation of Vegetable Oil

**M. A. Usman, T. O. Alaje, V. I. Ekwueme, and E. A. Awe**

*Department of Chemical Engineering, University of Lagos, Akoka-Yaba, 101017 Lagos, Nigeria*

Correspondence should be addressed to M. A. Usman, mawwal04@yahoo.com

Received 19 December 2011; Accepted 16 January 2012

Academic Editors: A. Auroux and N. Homs

Copyright © 2012 M. A. Usman et al. This is an open access article distributed under the Creative Commons Attribution License, which permits unrestricted use, distribution, and reproduction in any medium, provided the original work is properly cited.

Highly ordered mesoporous materials are opening the door to new opportunities in catalysis due to their extraordinary intrinsic features. In this study, Nickel was supported on highly ordered mesoporous silica (KIT-6) by the wet impregnation method, and its performance in the hydrogenation of edible vegetable oil was compared with that of Ni/Activated carbon prepared using the same method as well as with unsupported Nickel. The degree of conversion for the 50 : 50 Ni/KIT-6 was 81%, as compared to the 29% obtained with 50 : 50 Ni/Activated carbons. The conversion was found to improve with an increase in mass of supported Nickel on KIT-6 thus 20 : 80 Ni/KIT-6 and 30 : 70 Ni/KIT-6 produced conversions of 71% and 74%, respectively. Key among the benefits of KIT-6 when used as a support material is the very high surface area, open framework of the 3D bicontinuous interconnected channels, and the well-ordered mesopores which bestow on it an advanced mass transfer characteristics.

## 1. Introduction

Catalytic hydrogenation is a very important reaction in the synthesis of organic compounds which dates back to 1897 when Paul Sabatier, a French Chemist [1], discovered that the introduction of a trace of nickel metal enabled the addition of hydrogen to molecules of hydrocarbon compounds. Since then, it has been widely used in various fields, which include industrial hydrogenation processes such as the synthesis of methanol, liquid fuels, hydrogenated oils, cyclohexanol, and cyclohexane. In the food industry, hydrogenation is applied to process vegetable oils and fats [2]. Unsaturated vegetable fats and oils can be hydrogenated by the catalytic addition of hydrogen at the ethylenic linkages of their acids to produce saturated or partially saturated fats and oils of higher melting point. The most common forms are shortening, margarines, and the partially hydrogenated fats used for frying and in processed food. These fats are desirable for their melting point, which allows for high temperature cooking and frying.

With rare exception, no reaction below 480°C occurs between H<sub>2</sub> and organic compounds in the absence of metal catalysts [3]. The catalyst binds both the H<sub>2</sub> and the unsaturated substrate and facilitates their union. The catalytic cycle starts with oxidative addition of an H<sub>2</sub> molecule to

the metal centre to give a metal dihydride species and ends with reductive elimination of the product [4, 5]. Because these complexes are difficult to remove and reuse, numerous attempts have been made to anchor the catalysts on organic or inorganic supports to combine the advantages of homogeneous catalytic systems (high activity, high selectivity, and excellent reproducibility) with the advantages of heterogeneous catalytic systems (long life, recycling, and continuous application). For industrial purposes, unsupported catalysts are seldom employed since supported catalysts have many advantages over unsupported catalysts. One exception to this is Raney-type catalysts, which are effectively employed in industrial hydrogenations in unsupported states. In general, use of support allows the active component to have a large exposed surface area, which is particularly important in those cases where a high temperature is required or where the active component is very expensive. An active component may be incorporated with a carrier in various ways, such as, by deposition, impregnation, precipitation, coprecipitation, adsorption, or ion exchange. For these preparation methods catalyst pretreatment is often necessary, because the solid materials containing metal compounds in nonmetallic state can exhibit only low catalytic activity or be catalytically

inactive. Catalyst pretreatment involves the catalyst calcination, catalyst reduction, and the catalyst aging. Unlike homogeneous hydrogenation, which takes place on a well-defined single metal centre, heterogeneous hydrogenation proceeds over a vast surface of a metal cluster. This gives rise to a large number of interaction possibilities and variety of relevant and irrelevant species present on the surface during the reaction.

The catalytic characteristics are determined mainly by the major metal component. Nickel (Ni), cobalt (Co), copper (Cu), platinum (Pt), palladium (Pd), ruthenium (Ru), rhodium (Rh), osmium (Os), iridium (Ir), and rhenium (Re) are used most often, and each metal has its own activity and selectivity profile. Nickel is used extensively in hydrogenation since Sabatier's discovery of its activity. The preparation and activation of Ni catalysts have been studied by numerous investigators [6]. It is frequently used in skeletal form as Raney nickel, which is produced by leaching away alumina from alloy of Ni and aluminum. The hydrogenation of almost all the functional groups can be accomplished over some form of Raney nickel.

The primary role of the support is to finely disperse and stabilize small metallic particles and thus provides access to a much larger number of catalytically active atoms than in the corresponding bulk metal. The most conventional supports are acidic or basic oxides and different types of carbons which can have very different properties, like specific surface area, pore volume, acidities, electronic and geometrical properties. The most conventional oxide supports are alumina ( $\text{Al}_2\text{O}_3$ ) [7, 8] and silica ( $\text{SiO}_2$ ) [9, 10]. Basic magnesia ( $\text{MgO}$ ) [11, 12], a variety of reducible oxides, like titania ( $\text{TiO}_2$ ), ceric oxide ( $\text{CeO}_2$ ) [13, 14], zirconia ( $\text{ZrO}_2$ ) [15, 16], Gallia ( $\text{Ga}_2\text{O}_3$ ) [17, 18] and alloy forming oxides, that is, zinc oxide ( $\text{ZnO}$ ) [19], stannic oxide ( $\text{SnO}_2$ ) [20, 21] have also been studied in hydrogenation reactions. A comparison of different oxides in hydrogenations was performed with Ru [22], Pt [23], Pd [24], and Cu [25]. In general oxide supports can provide stronger interactions with the main metal than carbon. Additionally, the full reduction of the metal might be more difficult on an oxide than on carbon.

Zeolites and mesoporous materials, which exhibit structured ordering at the nanometer scale, have been used for a long time in petrochemical applications. Due to their channel system and shape selective properties, these materials have a potential for synthesis of fine chemicals. The use of metal/zeolite systems in the hydrogenation reactions is of course limited to molecules which are small enough to enter into the zeolite pores. Zeolites such as ZSM-5, dealuminated Y zeolite, and alkali zeolite beta have been used as supports in toluene hydrogenation [26], tetralin hydrogenation [27], and chemoselective hydrogenation of citronellal [28]. Mesoporous materials have tunable pore sizes between 2 and 10 nm, therefore they can be more suitable for hydrogenation of large organic molecules than zeolite materials. Mesoporous materials such as MCM-41, MCM-48, and SBA-15 have been used in hydrogenation of alkynes [29], hydrogenation of arene derivatives [30], hydrogenation of allyl alcohol [31], propene hydrogenation [32], and hydrogenation of dimethyl itaconate [33].

In this study, the performance of mesoporous silica KIT-6 as support for nickel catalyst in the hydrogenation of vegetable oil (groundnut oil) was investigated and compared with that of nickel on activated carbon. The two composites were prepared by wet impregnation method. The stability of Ni/KIT-6 as well as effects of different catalyst loading, temperature, and stirring speed on its performance was also investigated.

## 2. Materials and Methods

**2.1. Materials.** Ethanol (99.5%, Aldrich); Hydrochloric acid (37%, Sigma-Aldrich); Nickel Nitrate (98% J. K. Baker), Activated carbon (BDH, England (Product No. 33032), Wijs solution (J. K. Baker), Tetraethyl orthosilicate, TEOS (Sigma-Aldrich), N-butanol, Ethanol, poly(ethylene glycol)-block-poly(propylene glycol)-block-poly(ethylene glycol) (Sigma-Aldrich), zinc metal, Vegetable oil (groundnut oil). All the chemicals were used as received without further purification.

**2.2. Preparation of KIT-6 Support.** The mesoporous silica was synthesized following Kim's method [34]. Typically, 6 g Pluronic P123 (polyethylene oxide-polypropylene oxide-polyethylene oxide copolymer) was dissolved in 217 g of deionised water and 11.628 g of 37 wt% conc. HCl solution with stirring at 35°C. After complete dissolution, 6 g of butanol was added at once with vigorous stirring. After 1 h of stirring, 12.9 g of tetraethyl orthosilicate (TEOS) was added at once to the homogenous clear solution while still stirring. The mixture was left under vigorous and constant stirring for 24 h at 35°C. Afterwards, the mixture was placed in an oven at 100°C and left for 24 h under static conditions (in a closed polypropylene bottle). The solid product obtained after hydrothermal treatment was filtered while hot and dried at 100°C without washing. To complete the synthesis, the template was removed by extraction in an ethanol-HCl mixture; this was done by stirring the filtrate for 1-2 h in a mixture of 300-400 mL ethanol with 20-30 mL 37% conc. HCl followed by calcination in air at 550°C for 6 h.

**2.3. Procedure for the Synthesis of Catalyst and Hydrogenation Reaction.** Two sets of catalysts were prepared using activated carbon and KIT-6 as supports with the following weight ratios 50 wt% Ni/Activated carbon while the Ni/KIT-6 was in 50 wt% Ni/KIT-6, 30 wt% Ni/KIT-6, and 20 wt% Ni/KIT-6. The nickel nitrate was dissolved in distilled water at room temperature to form an aqueous solution which was added to the support in a dropwise form to impregnate it with the catalyst, the product was dried in an oven at 120°C for five hours followed by calcination in a muffle furnace for five hours at 500°C. The impregnated catalyst was then cooled and kept in an air-tight container pending the hydrogenation reaction.

The setup for the hydrogenation reaction consisted of two 500 mL conical flask connected with a hose. Hydrogen was produced in the first flask by adding 22 g of zinc metal to 60 mL 0.6 M HCl, this was used to purge the system for 15 minutes, the catalyst was also activated with hydrogen

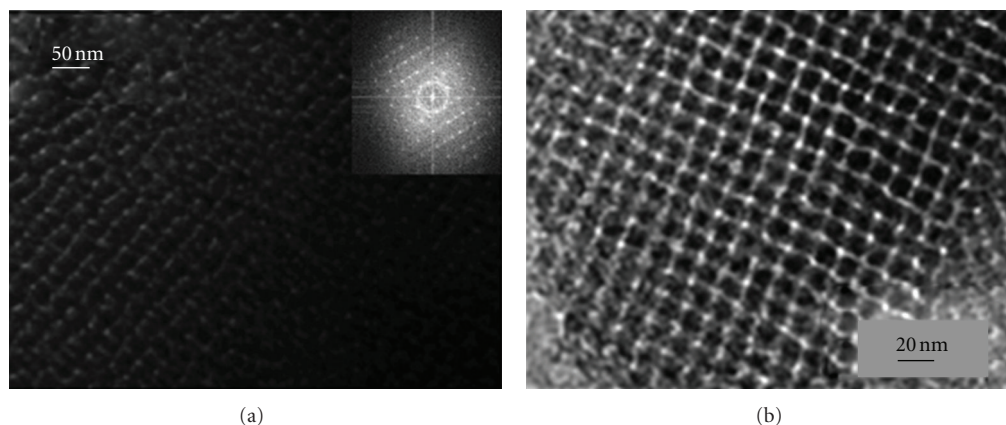


FIGURE 1: Transmission electron micrograph of the KIT-6 used. (Inset is the FFT.)

for 15 minutes, while activating the catalyst, the setup was maintained at a temperature between 310°C and 330°C. The reactions were carried out by allowing hydrogen into the second flask containing 10 mL of vegetable oil and 0.05 g of catalyst/support composite under vigorous stirring. The hose was filled with silica gel pellets to dry the wet hydrogen gas coming from the first flask, the two flasks were corked and all joints and connections tested for leakages. The reaction was carried out for 2 hours. Thereafter, the suspension was immediately decanted and filtered. The products were dried under vacuum and kept for further analysis. The catalysts were washed with solvent, dried and stored. The filtrates were kept in an air-tight container pending iodine value determination.

The morphology of the KIT-6 and the supported catalyst, namely, Ni/C and Ni/KIT-6, were examined using transmission electron microscopy (TEM) and a Hitachi X-650 scanning electron microanalyzer (SEM).

**2.4. Iodine Value Detection.** For a simple analysis, 0.2 grams of the fat was mixed with 20 mL Wijs solution and left in the dark for 30 minutes. To this was added 15 mL of 10% potassium iodide solution and 10 mL of deionized water. The final mixture was titrated against 0.1 M sodium thiosulfate (VI) solution. 1 mL of 0.1 M sodium thiosulfate solution = 0.01269 g of iodine.

The difference between a control titration and the titration with the fat present multiplied by this factor gave the mass of iodine absorbed by the oil.

In a typical procedure, the oil is treated with an excess of the Hanuš or Wijs solutions, which are, respectively, solutions of iodine monobromide (IBr) and iodine monochloride (ICl) in glacial acetic acid. Unreacted iodine monobromide (or monochloride) is reacted with potassium iodide, converting it to iodine, whose concentration can be determined by titration with sodium thiosulfate. The iodine number is thus calculated using the formula

$$IV = \frac{(B - S) \times N \times 12.69}{\text{mass of sample}}, \quad (1)$$

where IV is the iodine value; B is the titrant of the blank sample; S is the titrant of the sample; N is the normality of sodium thiosulfate.

**2.5. Effect of Temperature on the Degree of Conversion Using 30 wt%Ni/70 wt%KIT-6.** The effect of temperature on the degree of conversion was monitored at 100, 150, and 180°C using 30 wt%Ni/70 wt%KIT-6 following the method described for hydrogenation and iodine value detection in Sections 2.3 and 2.4, respectively.

### 3. Results and Discussion

Transmission electron micrograph of the mesoporous silica KIT-6 (Figure 1) reveals large domains of well-ordered pores. This attests to the highly ordered nature of the mesoporous silica material used. An important characteristic of the TEM is the uniform mesoporosity which is very evident from the top view of the pore structure. Equally obvious from the lateral view is the continuous and ordered nature of the channels. The inset Fourier transform infrared image further substantiates the fact that the pores are highly ordered.

Particles and aggregates can be observed in the SEM as shown in Figure 2. The particles from Ni/C appear smaller than those of Ni/KIT-6. Thus it would have been expected that Ni/C would have a higher activity, but the reverse is true. This can be due to the very high surface area of the KIT-6-ordered mesoporous silica coupled with well-ordered pore structure.

The iodine value for the crude vegetable oil was 80.00. There was a reduction in the iodine values of the hydrogenated variant and that was indicative of the level of hydrogenation achieved. The vegetable oil used for this work is derived from groundnut and has low iodine values and hence low unsaturation level. Due to these facts, the oil is less reactive and can be a good measure of catalyst efficiency, since they are difficult to hydrogenate.

Figure 3 reveals the performance of the different catalysts when used for a two hour hydrogenation of vegetable oil. Clearly, the Ni/KIT-6 catalysts exhibited a superior catalytic

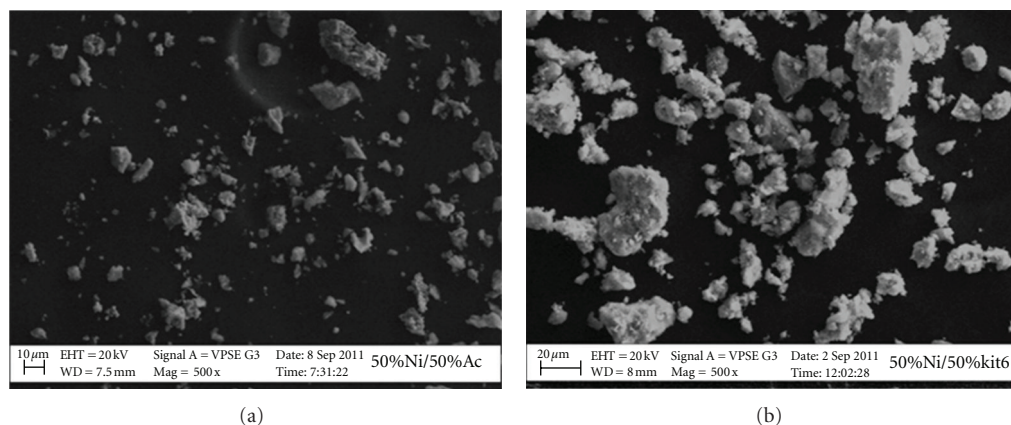


FIGURE 2: Scanning electron micrographs of supported catalysts ((a) Ni/C; (b) Ni/KIT-6).

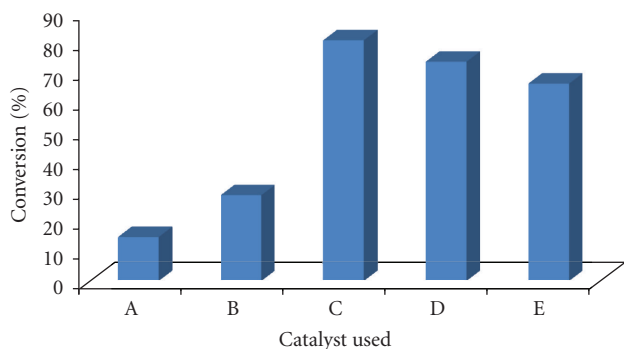


FIGURE 3: Performance of catalysts. (A) Nickel, (B) 50 : 50 Ni/ Activated carbon, (C) 50 : 50 Ni/KIT-6, (D) 30 : 70 Ni/KIT-6, and (E) 20 : 80 Ni/KIT-6 (wt %).

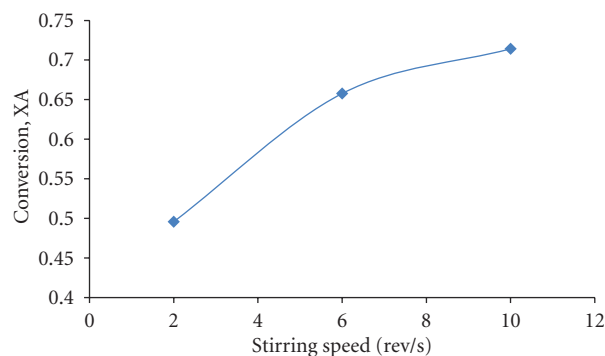


FIGURE 4: Effect of stirring speed on conversion at 180°C (using Ni/KIT-6).

activity compared with Ni/Activated carbon. This is evident even when a lower percentage of Nickel is deposited, as the 20 : 80 Ni/KIT-6 (wt%) with 66% conversion performed much better than the 50 : 50 Ni/Activated carbon (wt%) with 28% conversion. This can be ascribed to the very high surface area of the mesoporous silica, the large pores, and the highly ordered nature of the pores that allows for easy mass transfer of reactants and products in and out of the pores, respectively.

The lower catalytic activity of Ni catalyst supported on the microporous activated carbon (catalyst Ni/Activated Carbon) than that of Ni supported on the mesoporous materials (Ni/KIT-6) may be due to the effects of steric hindrance imposed by the molecular sizes of the reactants relative to the pore sizes of support.

The hydrogenation experiments were carried out in a batch-wise manner operating at atmospheric pressure between 100 and 180°C as shown in Figure 6, and the effect of stirring was studied in order to investigate the role of mass transfer. This was achieved by using stirrer speeds of 2, 6, 10 rev/sec as shown in Figure 4.

From the results, it is obvious that external mass transfer limitation is a factor to be considered seeing that the conversion increased with an increase in stirrer speed. This may

be explained by the fact that H<sub>2</sub> has to diffuse through the slurry of oil-catalyst into the pores of the heterogeneous catalysts before they can interact with the Nickel. The faster the stirring speed the easier an diffusion becomes and the greater the conversion. It also further lends credence to the fact that the catalysts are located in the pores of the support. The increase in conversion seems to diminish as the stirrer speed is increased further, perhaps pointing to the fact that a point may be attained when conversion will cease to increase as the stirrer speed increases, thus signifying absence of external mass transfer resistance.

Increasing the mass of the catalysts used boosts the number of Ni active sites available for hydrogenation and consequently results in a linear increase in conversion. This can be seen from Figure 5. However, the increase seems to be more pronounced at higher concentrations of catalyst.

The temperature dependency of the catalyst hydrogenation reaction is not surprising considering that based on the Arrhenius equation the activation energy is directly dependent on temperature and the higher the activation energy the greater the expected conversion.

The stability of catalyst performance is of extreme importance in industrial hydrogenations. An industrial catalyst must be stable against sintering and poisoning. The high

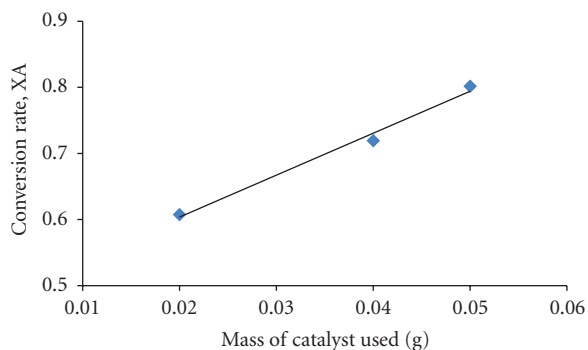


FIGURE 5: Influence of catalyst loading on the conversion rate at 180°C (using 30 : 70 wt% Ni/KIT-6) for a reaction time of 2 hours.

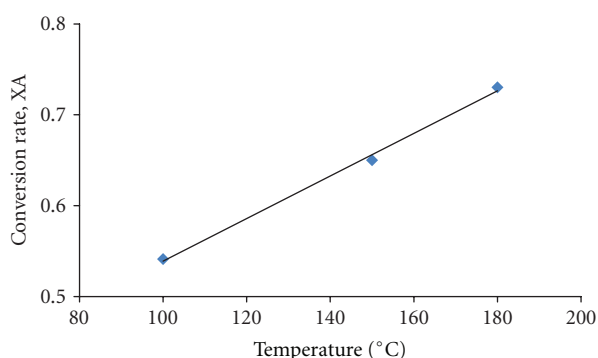


FIGURE 6: The influence of temperature on conversion.

stability of the Nickel deposited on KIT-6 is evident from Figure 7.

After the first run, the Ni/KIT-6 catalyst was recovered, washed with distilled water, dried at 120°C in air, and reused without further treatment. The reduction in catalytic activity of the reused Ni/KIT-6 was not too pronounced and even this can be ascribed to the fact that the mass of recovered catalyst was smaller than the mass of fresh catalyst. So it is reasonable to say that the activity is likely to have remained the same even after reuse. This makes the support highly recommended for industrial purposes as it will save the additional expense of having to use fresh catalyst for each run of hydrogenation.

#### 4. Conclusions

The Ni/KIT-6 catalysts demonstrated a much higher catalytic activity for the hydrogenation of vegetable oil in comparison with the Ni/Activated carbon and the unsupported Nickel catalyst. In addition to their higher activity, the Ni/KIT-6 catalysts also had the crucial advantage of being stable (i.e., it was reused) and resistant to leaching and poisoning. This can be ascribed to the higher surface area—larger pores as well as the highly ordered interconnected and intertwined cubic Ia3d structure of the pores. Compared with other ordinary Ni catalysts, Ni/KIT-6 catalysts exhibit higher catalytic activity because of the enhanced contact

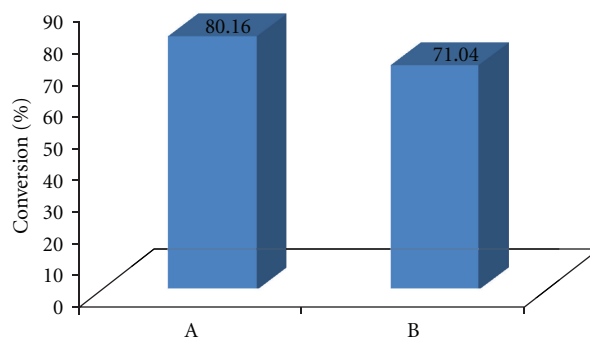


FIGURE 7: Catalytic activity of fresh and reused Ni/KIT-6. (A) Fresh 50 : 50 Ni/KIT-6. (B) Reused 50 : 50 Ni/KIT-6.

between the Ni metal and the catalyst support, together with the unblocked pores of the catalysts. Such intimate contact may favor a very close contact with the hydrogen gas, which greatly enhanced the transfer rate of hydrogen species. Therefore, more hydrogen could be adsorbed on the Ni/KIT-6 catalysts, which in turn enhanced its hydrogenation activity.

#### References

- [1] P. Sabatier and J.-B. Senderens, "New methane synthesis," *Annales de Chimie et de Physique*, vol. 4, pp. 319–323, 1905.
- [2] H. B. W. Patterson, *Hydrogenation of Fat and Oils*, Applied Science, New York, NY, USA, 1983.
- [3] S. Nishimura, *Handbook of Heterogeneous Catalytic Hydrogenation for Organic Synthesis*, John Wiley & Sons, New York, NY, USA, 2001.
- [4] T. Dwars and G. Oehme, "Complex-catalyzed hydrogenation reactions in aqueous media," *Advanced Synthesis and Catalysis*, vol. 344, no. 3-4, pp. 239–260, 2002.
- [5] H. U. Blaser, C. Malan, B. Pugin, F. Spindler, H. Steiner, and M. Studer, "Selective hydrogenation for fine chemicals: recent trends and new developments," *Advanced Synthesis and Catalysis*, vol. 345, no. 1-2, pp. 103–151, 2003.
- [6] P. Fouilloux, "The nature of raney nickel, its adsorbed hydrogen and its catalytic activity for hydrogenation reactions," *Applied Catalysis*, vol. 8, no. 1, pp. 1–42, 1983.
- [7] D. A. Echeverri, J. M. Marin, G. M. Restrepo, and L. A. Rios, "Characterization and carbonylic hydrogenation of methyl oleate over Ru-Sn/Al<sub>2</sub>O<sub>3</sub>: effects of metal precursor and chlorine removal," *Applied Catalysis A*, vol. 366, no. 2, pp. 342–347, 2009.
- [8] F. Hoxha, N. van Vegten, A. Urakawa, F. Krumeich, T. Mallat, and A. Baiker, "Remarkable particle size effect in Rh-catalyzed enantioselective hydrogenations," *Journal of Catalysis*, vol. 261, no. 2, pp. 224–231, 2009.
- [9] L. F. Chen, P. J. Guo, M. H. Qiao et al., "Cu/SiO<sub>2</sub> catalysts prepared by the ammonia-evaporation method: texture, structure, and catalytic performance in hydrogenation of dimethyl oxalate to ethylene glycol," *Journal of Catalysis*, vol. 257, no. 1, pp. 172–180, 2008.
- [10] H. G. Manyar, D. Weber, H. Daly et al., "Deactivation and regeneration of ruthenium on silica in the liquid-phase

- hydrogenation of butan-2-one,” *Journal of Catalysis*, vol. 265, no. 1, pp. 80–88, 2009.
- [11] S. Recchia, C. Dossi, N. Poli, A. Fusi, L. Sordelli, and R. Psaro, “Outstanding performances of magnesia-supported platinum-tin catalysts for citral selective hydrogenation,” *Journal of Catalysis*, vol. 184, no. 1, pp. 1–4, 1999.
- [12] L. Sordelli, R. Psaro, G. Vlačić et al., “EXAFS studies of supported Rh-Sn catalysts for citral hydrogenation,” *Journal of Catalysis*, vol. 182, no. 1, pp. 186–198, 1999.
- [13] F. Fajardie, J. F. Tempere, G. Djega-Mariadassou, and G. Blanchard, “Benzene hydrogenation as a tool for the determination of the percentage of metal exposed on low loaded ceria supported rhodium catalysts,” *Journal of Catalysis*, vol. 163, no. 1, pp. 77–86, 1996.
- [14] B. Campo, G. Santori, C. Petit, and M. Volpe, “Liquid phase hydrogenation of crotonaldehyde over Au/CeO<sub>2</sub> catalysts,” *Applied Catalysis A*, vol. 359, no. 1-2, pp. 79–83, 2009.
- [15] P. Claus, A. Bruckner, C. Mohr, and H. Hofmeister, “Supported gold nanoparticles from quantum dot to mesoscopic size scale: effect of electronic and structural properties on catalytic hydrogenation of conjugated functional groups,” *Journal of the American Chemical Society*, vol. 122, no. 46, pp. 11430–11439, 2000.
- [16] A. B. Gaspar, G. R. dos Santos, R. D. Costa, and M. A. P. da Silva, “Hydrogenation of synthetic PYGAS—effects of zirconia on Pd/Al<sub>2</sub>O<sub>3</sub>,” *Catalysis Today*, vol. 133–135, pp. 400–405, 2008.
- [17] E. Gebauer-Henke, J. Grams, E. Szubiakiewicz, J. Farbotko, R. Touroude, and J. Rynkowski, “Pt/Ga<sub>2</sub>O<sub>3</sub> catalysts of selective hydrogenation of crotonaldehyde,” *Journal of Catalysis*, vol. 250, no. 2, pp. 195–208, 2007.
- [18] F. Dominguez, J. Sanchez, G. Arteaga, and E. Choren, “Gallia as support of Pt in benzene hydrogenation reaction,” *Journal of Molecular Catalysis A*, vol. 228, no. 1-2, pp. 319–324, 2005.
- [19] B. Nohair, C. Especel, G. Lafaye, P. Marecot, L. C. Hoang, and J. Barbier, “Palladium supported catalysts for the selective hydrogenation of sunflower oil,” *Journal of Molecular Catalysis A*, vol. 229, no. 1-2, pp. 117–126, 2005.
- [20] K. Liberková and R. Touroude, “Performance of Pt/SnO<sub>2</sub> catalyst in the gas phase hydrogenation of crotonaldehyde,” *Journal of Molecular Catalysis A*, vol. 180, no. 1-2, pp. 221–230, 2002.
- [21] K. Liberková, R. Touroude, and D. Y. Murzin, “Analysis of deactivation and selectivity pattern in catalytic hydrogenation of a molecule with different functional groups: crotonaldehyde hydrogenation on Pt/SnO<sub>2</sub>,” *Chemical Engineering Science*, vol. 57, no. 13, pp. 2519–2529, 2002.
- [22] B. Bachiller-Baeza, A. Guerrero-Ruiz, and I. Rodríguez-Ramos, “Ruthenium-supported catalysts for the stereoselective hydrogenation of paracetamol to 4-*trans*-acetamidocyclohexanol: effect of support, metal precursor, and solvent,” *Journal of Catalysis*, vol. 229, no. 2, pp. 439–445, 2005.
- [23] J. Kijenski, P. Winiarek, T. Paryjczak, A. Lewicki, and A. Mikolajska, “Platinum deposited on monolayer supports in selective hydrogenation of furfural to furfuryl alcohol,” *Applied Catalysis A*, vol. 233, no. 1-2, pp. 171–182, 2002.
- [24] F. Pinna, F. Menegazzo, M. Signoretto, P. Canton, G. Fagherazzi, and N. Pernicone, “Consecutive hydrogenation of benzaldehyde over Pd catalysts: influence of supports and sulfur poisoning,” *Applied Catalysis A*, vol. 219, no. 1-2, pp. 195–200, 2001.
- [25] A. Saadi, Z. Rassoul, and M. M. Bettahar, “Gas phase hydrogenation of benzaldehyde over supported copper catalysts,” *Journal of Molecular Catalysis A*, vol. 164, no. 1-2, pp. 205–216, 2000.
- [26] A. Masalska, “Ni-loaded catalyst containing ZSM-5 zeolite for toluene hydrogenation,” *Applied Catalysis A*, vol. 294, no. 2, pp. 260–272, 2005.
- [27] A. S. Rocha, E. L. Moreno, G. P. M. da Silva, J. L. Zotin, and A. C. Faro, “Tetralin hydrogenation on dealuminated Y zeolite-supported bimetallic Pd-Ir catalysts,” *Catalysis Today*, vol. 133–135, pp. 394–399, 2008.
- [28] M. L. Kantam, B. P. C. Rao, B. M. Choudary, and B. Sreedhar, “Selective transfer hydrogenation of carbonyl compounds by ruthenium nanoclusters supported on alkali-exchanged zeolite beta,” *Advanced Synthesis and Catalysis*, vol. 348, no. 14, pp. 1970–1976, 2006.
- [29] A. Papp, A. Molnar, and A. Mastalir, “Catalytic investigation of Pd particles supported on MCM-41 for the selective hydrogenations of terminal and internal alkynes,” *Applied Catalysis A*, vol. 289, no. 2, pp. 256–266, 2005.
- [30] M. Boutros, F. Launay, A. Nowicki et al., “Reduced forms of Rh(III) containing MCM-41 silicas as hydrogenation catalysts for arene derivatives,” *Journal of Molecular Catalysis A*, vol. 259, no. 1-2, pp. 91–98, 2006.
- [31] Y. J. Jiang and Q. M. Gao, “Heterogeneous hydrogenation catalyses over recyclable Pd(0) nanoparticle catalysts stabilized by PAMAM-SBA-15 organic-inorganic hybrid composites,” *Journal of the American Chemical Society*, vol. 128, no. 3, pp. 716–717, 2006.
- [32] M. Boualleg, J. M. Basset, J. P. Candy et al., “Regularly distributed and fully accessible Pt nanoparticles in silica pore channels via the controlled growth of a mesostructured matrix around Pt colloids,” *Chemistry of Materials*, vol. 21, no. 5, pp. 775–777, 2009.
- [33] A. Crosman and W. F. Hoelderich, “Enantioselective hydrogenation over immobilized rhodium diphosphine complexes on aluminated SBA-15,” *Journal of Catalysis*, vol. 232, no. 1, pp. 43–50, 2005.
- [34] T. Kim, F. Kleitz, B. Paul, and R. Ryoo, “MCM-48-like large mesoporous silicas with tailored pore structure: facile synthesis domain in a ternary triblock copolymer-butanol-water system,” *Journal of the American Chemical Society*, vol. 127, no. 20, pp. 7601–7610, 2005.



# Hindawi

Submit your manuscripts at  
<http://www.hindawi.com>

